Available online at www.sciencedirect.com

ScienceDirect

Catalysis Today 131 (2008) 285–291

CATALYSIS TODAY

www.elsevier.com/locate/cattod

# Effect of different calcination environments on the vanadium phosphate catalysts for selective oxidation of propane and *n*-butane

Y.H. Taufiq-Yap *, C.S. Saw

*Putra Laboratory for Catalysis Science and Technology, Department of Chemistry, Faculty of Science, Universiti Putra Malaysia, 43400 UPM Serdang, Selangor, Malaysia*

---

**Abstract**

Vanadium phosphate catalysts were synthesized via $VOPO_4{\cdot}2H_2O$ and were calcined in two different hydrocarbon reaction environments, *i.e.* *n*-butane/air and propane/air. Both catalysts are denoted VPDB and VPDP, respectively. Both catalysts exhibited a good crystalline with characteristic peaks of pyrophosphate phase. However, the peaks for VPDP are shown to be more prominent than those of VPDB. BET surface area showed that VPDB gave higher surface area (23 $m^2\,g^{-1}$) compared to VPDP (18 $m^2\,g^{-1}$). The average V valence state for VPDP is 4.08 and the higher V valence state for VPDB is 4.26 due to higher amount of $V^{V}$ for VPDB. Furthermore 14.2% of $V^{III}$ was found for VPDP but none for VPDB. SEM micrographs clearly revealed that the morphologies of both catalysts composed of plate-like crystallite that was arranged into the characteristic of rosette cluster. However, the catalyst calcined in *n*-butane/air environment (VPDB) resulted in an increment of the amount of plate-like crystal formed in the rosette rosebud agglomerates. TPR in $H_2$ profiles of both catalysts gave two reduction peaks corresponding to two kinetically different oxygen species which were associated with $V^{V}$ and $V^{IV}$ phases, respectively. VPDB removed larger amount of active oxygen species linked to $V^{IV}$ phase which eventually caused a higher conversion rate in the selective oxidation of *n*-butane and propane to maleic anhydride and acrylic acid, respectively.

*Keywords:* VPO; *n*-Butane oxidation; Propane oxidation; Maleic anhydride; Acrylic acid

---

## 1. Introduction

The most active phase of VPO catalysts for synthesis of MA is made up of a well-crystallized $(VO)_2P_2O_7$ which is considered to possess unique structural and surface features to allow the activation of alkane [1,2]. This phase is generally generated by a long-term calcination of the precursor, $VOHPO_4{\cdot}0.5H_2O$ prepared via reduction of $VOPO_4{\cdot}2H_2O$ using isobutanol as reducing agent followed by treatment in a reaction environment. Transformation of precursor to active phase can be affected by the temperature, time and atmosphere of treatment [1].

The surface chemistry and bulk properties of the active VPO catalysts change with the time of calcination and with the calcination condition [4]. The composition of the VPO surface is complex as crystalline phases other than the main phase vanadyl pyrophosphate are often observed and disordered phases are also found. The capability of VPO system to form different phases with similar structures often leads to a multiphase system and all these phases can be transformed easily into each other enhanced the complexity of the VPO catalysts. Different phases showed different catalytic performance in selective oxidation of *n*-butane. A number of previous studies [2,5] suggested that a combination of vanadyl pyrophosphate along with patches of $VOPO_4$ phases play an important role in the selective oxidation of *n*-butane. However, very little has been reported concerning the catalyst active phases or active sites of the VPO catalyst in selective oxidation of propane. Therefore, the nature of the active sites, the preferred composition of the catalyst and the role of the $V^{V}$ and $V^{III}$ phases remain to be a fascinating topic for study.

In the present study, we investigate the influence of calcination agents (*n*-butane/air and propane/air) on the catalytic performance of the VPO catalysts prepared from $VOPO_4{\cdot}2H_2O$ for partial oxidation of *n*-butane and propane. The changes in the physical and chemical properties of the VPO catalysts calcined in

---

* Corresponding author. Tel.: +60 3 89466809; fax: +60 3 89466758.
*E-mail address:* yap@fsas.upm.edu.my (Y.H. Taufiq-Yap).

0920-5861/$ – see front matter © 2007 Elsevier B.V. All rights reserved.
doi:10.1016/j.cattod.2007.10.091

two different conditions are systematically observed by X-ray diffraction, redox titration, ICP-AES, $N_2$ adsorption–desorption isotherms, scanning electron microscopy (SEM) and $H_2$-TPR. Furthermore, their catalytic performances are discussed in relation to the reactivity of the lattice oxygen and the vanadium species present in the samples.

## 2. Experimental

### 2.1. Catalysts—preparation

The catalysts were prepared via dihydrate method. Vanadium pentoxide, $V_2O_5$ (15.0 g from Fluka), was suspended by rapid stirring into a mixture of *o*-$H_3PO_4$ 60 mL, 85% from Merck (71.75 $cm^3$) and water (360 $cm^3$). The vanadium oxide–acid mixture was stirred and refluxed for 24 h at 393 K. The mixture was then cooled to room temperature. The yellow solid was recovered by filtration, washed sparingly with water and oven dried at 383 K for 24 h. $VOPO_4{\cdot}2H_2O$ was then refluxed with isobutanol (1 g/20 mL) for 21 h and the solid product was recovered by filtration and oven dried at 383 K for 21 h to obtain the precursor, $VOHPO_4{\cdot}0.5H_2O$, denoted VPDpre. The resulting precursor, which was shown to be a well-crystallized $VOHPO_4{\cdot}0.5H_2O$ by XRD analysis, was then calcined under a flow of propane/air mixture (1% propane in air) at 673 K for 36 h (denoted VPDP) and under a flow of *n*-butane/air (0.75% *n*-butane in air) for 75 h (denoted VPDB).

### 2.2. Catalysts—characterization

The total surface area of the catalysts was measured by BET (Brunauer–Emmer–Teller) method using $N_2$ adsorption at 77 K. This was done by using ThermoFinnigan Sorptomatic 1990 nitrogen adsorption–desorption analyzer.

The average oxidation states of vanadium in all the samples were determined by the method described by Niwa and Murakami [6].

The X-ray diffraction (XRD) analyses were carried out using a Shimadzu diffractometer model XRD 6000 employing Cu Kα radiation to generate diffraction patterns from powder crystalline samples at ambient temperature.

The bulk chemical composition was determined by using a sequential scanning inductively coupled plasma-atomic emission spectrometer (ICP-AES) Perkin-Elmer Emission Spectrometer model Plasma 1000.

SEM was done using a Jeol JSM-6400 electron microscope. The samples were coated with gold using a sputter coater.

TPR (temperature-programmed reduction) analysis was done using a ThermoFinigan TPDRO 1110 apparatus utilizing a thermal conductivity detector (TCD).

### 2.3. Catalytic oxidation of propane to acrylic acid

The oxidation of propane to acrylic acid was carried out at 673 K in a fixed bed multitubular reactor with a standard volume of catalyst (0.5 mL). A feedstock containing propane, oxygen, nitrogen and steam (ratio = 1/2/18/9) with GHSV = 1200 $h^{-1}$ was introduced to the reactor. The products were then fed via heated lines to an on-line gas chromatography for analysis.

### 2.4. Catalytic oxidation of *n*-butane to maleic anhydride

The oxidation of *n*-butane was carried out in a microreactor with a standard mass of catalyst (250 mg). The gases *n*-butane and air were fed to the reactor via calibrated mass flow controllers to give a feedstock composition of 1.5% *n*-butane in air. The products were then fed via heated lines to an on-line gas chromatograph for analysis. The reactor comprised a stainless steel tube with the catalyst held in place by plugs of quartz wool. A thermocouple was located in the centre of the catalyst bed and temperature control was typically $\pm 1\ ^\circ C$. Carbon mass balances of $\geq 97\%$ were typically observed.

## 3. Results and discussion

### 3.1. X-ray diffraction (XRD) analysis

The XRD pattern of the precursor, VPDpre (Fig. 1) only shows the characteristic reflections of vanadyl hydrogen phosphate hemihydrate ($VOHPO_4{\cdot}0.5H_2O$), with peaks at $2\theta = 15.5^\circ$, $19.6^\circ$, $24.14^\circ$, $27.0^\circ$ and $30.4^\circ$ [12]. The peaks at $2\theta = 15.5^\circ$ and $30.4^\circ$ corresponds to (0 0 1) and (1 3 0) reflections, respectively, and the (1 3 0) reflection was the dominant feature in the precursor which is the characteristic for the precursor prepared by using dihydrate method [7].

For VPDP and VPDB catalysts, the XRD patterns (Fig. 1) show similar diffraction pattern composed of a well-crystallized $(VO)_2P_2O_7$ phase with three main characteristic peaks appeared at $2\theta = 22.8^\circ$, $28.4^\circ$ and $29.8^\circ$, which correspond to (0 2 0), (2 0 4) and (2 2 1) planes, respectively.

All three peaks for the catalyst calcined in propane/air condition for VPDP are shown to be more prominent as compared to the 75 h *n*-butane/air calcined counterpart VPDB. In fact, catalyst calcined under *n*-butane/air is less crystalline compared with the catalyst calcined under propane/air stream. The development of the crystalline structure and/or

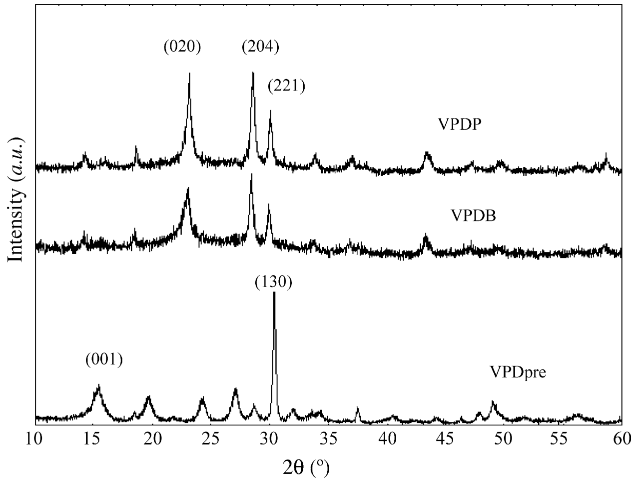

Fig. 1. XRD patterns of VPDpre, VPDB and VPDP.

transformation of the surface morphology is not only dependent upon duration of calcination but is also affected by the calcination atmosphere.

The (0 2 0) peak at $2\theta = 22.8^\circ$ for VPDP was shown to be more intense as compared with the same peak of the VPDB. It has been widely accepted that this (0 2 0) plane is active for the selective oxidation of *n*-butane [1], which leads to the expectation that with highly exposure of this (0 2 0) plane, VPDP show better desired product selectivity in the partial oxidation process than VPDB does.

The (0 2 0) and (2 0 4) planes were the most intense peaks for propane/air calcined catalyst, VPDP. This result suggests that the dominant surface of VPDP crystals was composed of (1 0 0) and (0 1 1) layers, respectively. However, the most dominant surface for *n*-butane/air calcined catalyst, VPDB, was the (0 1 1) layer because the most intense peak for the catalyst was observed at $2\theta = 28.4^\circ$ which corresponded to the (2 0 4) plane.

### 3.2. BET surface area measurement

The catalyst calcined in butane/air mixture (VPDB) gave higher BET surface area ($23\,m^2\,g^{-1}$) than the propane/air calcined counterpart, VPDP ($18\,m^2\,g^{-1}$). It increased with the reduction strength of the calcination atmospheres. As in the XRD diffraction patterns (Fig. 1), VPDP catalyst appears to have more intense (0 2 0) reflection than VPDB but the total surface area for VPDP was lower than VPDB. This demonstrates that the exposure of the (0 2 0) plane is not the only factor that lead to the increment of the total surface area. The amount of platelets present in the VPO crystalline structure and the degree of isolation for the platelets should also be considered. Vanadyl pyrophosphate is believed to have a layered structure in which these layers are interconnected in a tridimensional structure by weaker bonding, such as H bonding of phosphates. The cleavage of such structural characteristic may also increase the total surface area.

### 3.3. Chemical analysis and redox titration

The P/V atomic ratios, the average oxidation number of the vanadium and percentage of $V^{III}$, $V^{IV}$ and $V^{V}$ oxidation state are summarized in Table 1. The P/V atomic ratios for both samples obtained are not much different, 1.09 and 1.08 for VPDP and VPDB, respectively. Slightly excessive of phosphorus somehow helps stabilize the $V^{IV}$ oxidation state and limits the overoxidation of $(VO)_2P_2O_7$ to $VOPO_4$ both in the reactant's atmosphere and in air. The P/V ratio for both catalysts is in good agreement with those reported for industrial catalysts. Cavani et al. [8] also reported that P/V ratio is one of the key factors in catalyst preparation to avoid the oxidation of $(VO)_2P_2O_7$ and/or of the intermediate amorphous phase to a $V^V$ phosphate. However, it seems clear from the results obtained that the P/V atomic ratios did not depend strongly upon the duration of calcination and/or calcination atmosphere. The preparation route of the VPO catalysts appears to be more important in determining the P/V ratio of the catalysts.

Table 1
P/V ratios, average oxidation numbers and percentages of $V^{III}$, $V^{IV}$ and $V^{V}$ oxidation states present in VPDP and VPDB

| Catalyst | P/V ratio | Average oxidation number | $V^V$ (%) | $V^{IV}$ (%) | $V^{III}$ (%) |
|---|---|---|---|---|---|
| VPDP | 1.09 | 4.08 | 9.8 | 76.0 | 14.2 |
| VPDB | 1.08 | 4.26 | 26.0 | 74.0 | 0 |

The average oxidation number of vanadium for VPDP and VPDB is 4.08 and 4.26, respectively. The result reflects that oxidized phase such as $VOPO_4$ may exist in the VPDB but this corresponding oxidized phase is not detected by the XRD. However, this is not surprising because the XRD has been reported to be not sensitive enough to detect the small amount of $VOPO_4$ in $(VO)_2P_2O_7$ by Cavani et al. [8]. They had proved that there might be as high as 20% of $VOPO_4$ in addition to $(VO)_2P_2O_7$ with no clear modification of the XRD pattern.

The result shows that different calcination atmosphere did not affect the $V^{IV}$ composition in both catalysts. An increased of the $V^V$ was detected in catalyst calcined in *n*-butane/air atmosphere, VPDB with 26% of $V^V$ species compared to only 9.8% for VPDP catalyst. Previous studies had demonstrated that $(VO)_2P_2O_7$ alone is not the active phase for selective oxidation of *n*-butane to MA, a suitable $V^{IV}/V^V$ balance is required for the best performance of this material [9]. However, the effect is very complex and the perfect $V^{IV}/V^V$ balance to achieve the best performance in selective oxidation of light alkanes is still not clear. Another interesting point to be highlighted here is that the observation of $V^{III}$ species in the VPDP catalyst. This species was not found in the catalyst calcined in *n*-butane/air mixture environment (VPDB).

For VPDP catalyst, there co-existed $V^{III}$, $V^{IV}$ and $V^V$ phases. As the $V^{IV}$ concentration for both catalysts were almost the same, *i.e.* 76% and 74% for VPDP and VPDB, respectively. This suggests that the direct reduction of $V^V$ to $V^{III}$ dominates the reduction process during the propane/air calcination. The role of $V^{III}$ was also not well understood in both *n*-butane and propane oxidation. Much less information is available for VPO catalysts containing $V^{III}$ species. Gai and Kourtakis [10] and Cavani et al. [8] suggested that the presence of $V^{III}$ species might enhances the specific activity in *n*-butane oxidation.

### 3.4. Scanning electron microscopy (SEM)

The morphology image of the precursor (VPDpre) is shown as rosebud shape in Fig. 2. Figs. 3 and 4 show the morphologic images of the VPDP and VPDB catalysts, respectively. Both catalysts show plate-like crystals which agglomerated into the characteristics of rosebud shape clusters. These rosebud shapes agglomerates are made up of $(VO)_2P_2O_7$ platelets that preferentially expose the (0 2 0) crystal plate. The amount of the platelet in the characteristic rosebud shape agglomerates was discerned to be different for both catalysts.

Catalyst calcined in *n*-butane/air environment resulted in an increment of the amount of plate-like crystal formed in the rosette rosebud agglomerates as compared to VPDP. The

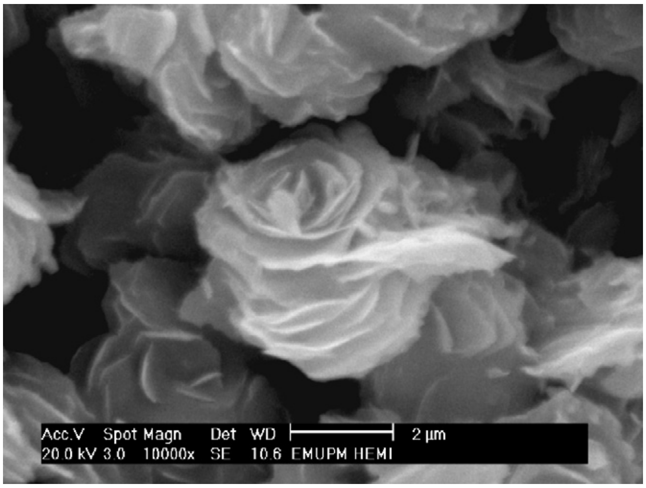

Fig. 2. SEM micrograph of precursor, VPDpre.

difference between the amounts of plate-like crystals seems to support that VPDB shows higher total surface area. Nevertheless, the degree of isolation for these characteristic rosebud-type agglomerates is affected by propane/air environment.

This observation suggested that the oxidizing strength of the calcination gases affects the morphology of the calcined catalysts. Abon et al. [11] reported the increased of the crystallinity of $(VO)_2P_2O_7$ phase would change the morphology of the catalyst particles and bring about the formation of more split agglomerates. The SEM micrograph of VPDP was also in good agreement with the result obtained from the XRD patterns where the increase of (0 2 0) reflection intensity would bring out the formation of more split $(VO)_2P_2O_7$.

### 3.5. Temperature-programmed reduction in $H_2$/Ar ($H_2$-TPR)

Fig. 5 shows the TPR profiles for VPDP and VPDB catalysts in $H_2$/Ar stream (5% $H_2$ in Ar, 1 bar, 25 $cm^3$ $min^{-1}$) using a fresh sample of catalyst and raising the temperature from ambient to ~1123 K at a heating rate of 5 K $min^{-1}$ in that stream. From this analysis, the information as to the nature and the oxidizing species available from the catalysts could be obtained. The peak maxima temperatures, the amount of removed oxygen and the derived reduction activation energies are summarized in Table 2.

Fig. 3. SEM micrograph of VPDP catalyst.

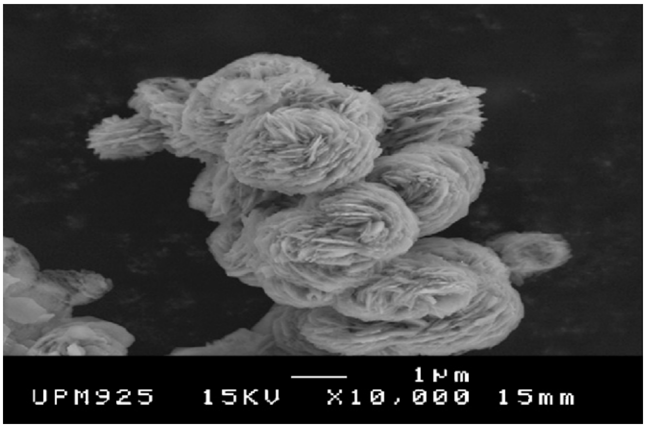

Fig. 4. SEM micrograph of VPDB catalyst.

The reduction profiles of vanadyl pyrophosphate catalyst prepared via dihydrate method and calcined in *n*-butane/air mixture environment, VPDB, was characterized by three reduction peaks maxima, α, β and γ occurred at 852, 1043 and 1141 K, respectively. However, the introduction of propane/air calcination in this study shifted the two reduction peaks, α and β peaks, towards remarkably lower temperatures at 752 and 952 K, whereas the γ peak for both catalysts remained at ~1140 K.

A close examination of these two reduction peaks (at the range of 500–850 K) shows that VPDB gave a slightly better reducibility compared to VPDP. This result indicated that VPDB possesses higher labile and more reactive lattice oxygen at lower temperature which will enhance the catalytic performance of the catalysts for the selective oxidation of alkanes.

The reduction activation energies for VPDP catalyst were calculated for the peaks maxima (Table 2): (i) 126, (ii) 159 and (iii) 191 kJ $mol^{-1}$ at 752, 952 and 1142 K, respectively,

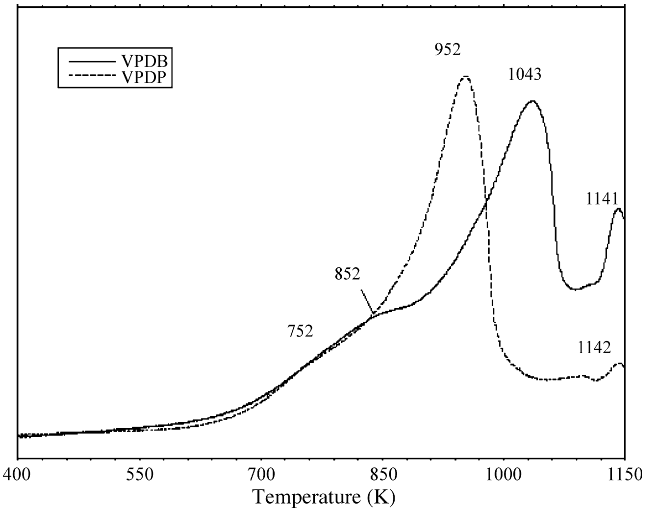

Fig. 5. TPR profiles for VPDP and VPDB catalysts.

Table 2
Amount of oxygen removed and reduction activation energies obtained by temperature-programmed reduction of $H_2$ with VPDP and VPDB

| Catalysts[a] | $T_{max}$ (K) | Reduction activation energy $E_r$ (kJ mol$^{-1}$) | $O_2$ atom removed from the catalysts ($\times 10^{-3}$ mol g$^{-1}$) | $O_2$ Atom removed from the catalysts ($\times 10^{21}$ atom g$^{-1}$) | Coverage[b] ($\times 10^{15}$ atom cm$^{-2}$) |
|---|---|---|---|---|---|
| VPDP | | | | | |
| 1 | 752 | 126 | 0.38 | 0.23 | 1.27 |
| 2 | 952 | 159 | 2.02 | 1.22 | 6.74 |
| 3 | 1142 | 191 | 0.03 | 0.02 | 0.11 |
| Total $O_2$ atom removed | | | 2.43 | 1.47 | 8.12 |
| VPDB | | | | | |
| 1 | 852 | 142 | 1.22 | 0.74 | 3.19 |
| 2 | 1043 | 174 | 2.61 | 1.57 | 6.77 |
| 3 | 1141 | 191 | 0.41 | 0.24 | 1.03 |
| Total $O_2$ atom removed | | | 4.24 | 2.55 | 10.99 |

[a] Surface area: VPDP = 18 m$^2$ g$^{-1}$ and VPDB = 23 m$^2$ g$^{-1}$.

[b] The "coverage" is calculated by dividing the number of oxygen atoms removed (atom g$^{-1}$) by the specific surface area.

whereas, the reduction activation energies obtained for VPDB catalyst are (i)142, (ii) 174 and (iii) 191 kJ mol$^{-1}$ at 852, 1043 and 1141 K, respectively.

### 3.6. Catalytic oxidation of propane

Both catalysts (VPDP and VPDB) were tested for propane oxidation to acrylic acid at 673 K, where this temperature being a typical operating temperature for VPO catalysts (Table 3). It is clear that propane/air calcined VPO catalyst, VPDP generally favoured higher selectivity of AA. VPDB was found to be more active with 14.1% of propane conversion, while only 7.9% of propane conversion rate were obtained by VPDP. This is in good agreement with the reduction behaviour of both catalysts discussed earlier. Indeed many papers reported that the VPO catalysts containing discrete amounts of $V^V$ sites have in general a better catalytic performance in the oxidation of *n*-butane than the catalysts which exclusively contain $V^{IV}$ sites [12]. Han et al. [13] also reported that the presence of a minor $VOPO_4$ ($V^V$) phase in $(VO)_2P_2O_7$ was shown to be effective for propane oxidation. Our data clearly indicate that with the combination of minor $V^V$ sites in the bulk of the vanadyl pyrophosphate, the activity of the catalyst was enhanced (Fig. 6). The selectivity towards acrylic acid (AA) of VPDP (81.5%) at 673 K was found significantly higher than VPDB (57.7%). This indicates that the catalysts that calcined in the propane/air stream are more selective than the *n*-butane calcined catalysts. The difference may be due to the presence of $V^{III}$ in the propane/air calcined catalyst, VPDP. The relationship between selectivity towards AA and percentage of $V^{III}$ species for both catalysts was examined (Fig. 7). This figure clearly showed a trend of increasing percentage of selectivity towards AA with an increase of $V^{III}$ species percentage. This behaviour confirms the role of the $V^{III}$ species, which is particularly improving the selectivity towards AA in propane oxidation and well agreed with our previous observation [14]. The increase in selectivity lowers the contribution of the consecutive reaction of acrylic acid combustion. The enhancement of acrylic acid (AA) selectivity is balanced by the decrease of $CO_x$ selectivity.

Table 3
The catalytic performance of VPDP and VPDB in propane oxidation

| Catalyst | Conversion of propane (%) | Product selectivity (%) | | |
|---|---|---|---|---|
| | | AA | CO | $CO_2$ |
| VPDP | 7.9 | 81.5 | 0 | 2.2 |
| VPDB | 14.1 | 57.5 | 17.9 | 9.6 |

Morphologic structure of the VPO catalysts also affected the catalytic performance of the catalysts in propane oxidation to AA. Our catalysts which in rosette shape clusters show higher AA selectivity (81.5% and 57.7% for VPDP and VPDB, respectively) compared to those which mainly comprised small lamellae. A higher AA selectivity achieved by our catalysts also can be explained by the high development of the $(VO)_2P_2O_7$. The *n*-butane/air and propane/air stream modified the surface structure of VPO catalysts as seen by comparing the SEM micrograph for both catalysts. The more agglomerated plate-like crystal of VPDB could be one of the reasons for the improved activity of the catalyst. SEM micrograph of VPDP showed plate-like crystalline on the surface of the catalyst is more isolated and the improved AA selectivity seem directly propositional with the degree of crystalline isolation in the catalysts.

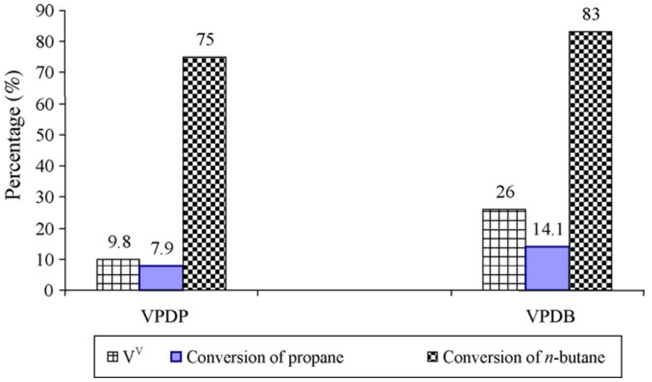

Fig. 6. The amount o f $V^V$ and activity relationship of VPDP and VPDB catalysts.

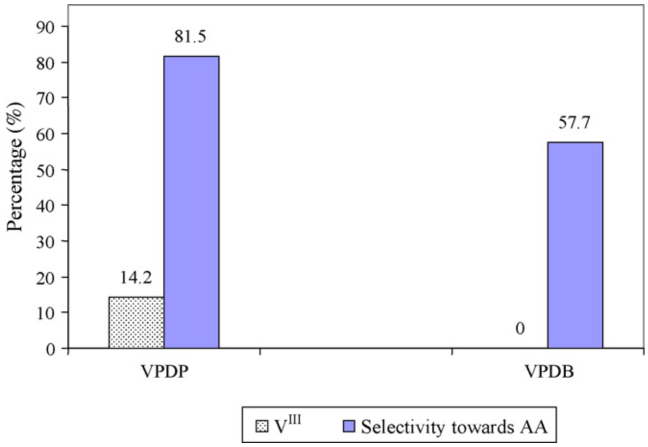

Fig. 7. The relation between the selectivity towards AA (%) and the percentage of $V^{III}$ (%) of VPDP and VPDB catalysts in propane oxidation.

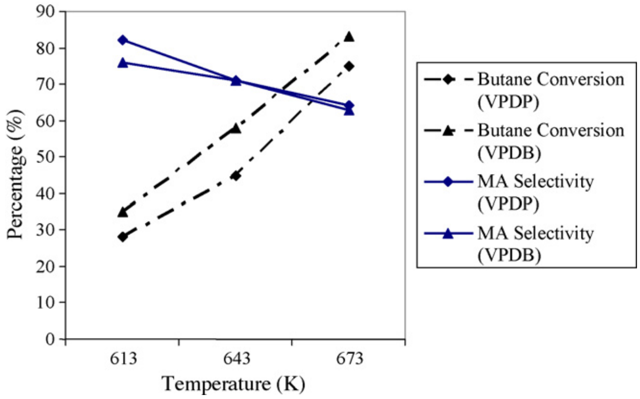

Fig. 8. The catalytic performance of VPO catalysts (VPDP and VPDB) as a function of the reaction operating temperature in $n$-butane oxidation.

As reported earlier [3], the catalytic performance of VPO is primarily dependent upon the catalyst surface area. Higher total surface area obtained is mostly associated with the high development of the $(VO)_2P_2O_7$ phase. In our case, the $n$-butane/air calcined catalyst, VPDB (23 $m^2\ g^{-1}$) was found to be more active with 14.1% conversion than the propane/air calcined counterpart, VPDP (18 $m^2\ g^{-1}$) (Fig. 8). The propane/air calcined catalyst, VPDP was shown to inhibit further oxidation of the intermediate and/or the desired product. No CO could be detected by on-line GC and the selectivity for $CO_2$ was only about 2.2% (Table 3). Beside surface area, the availability of highly active oxygen species ($O^-$) associated with $V^{IV}$ also plays the main role. Recently, one of us had observed a good correlation between anion $O^-$ and $n$-butane conversion [15]. This again shows that $O^-$ also plays an important role in determining the catalytic activity of propane oxidation.

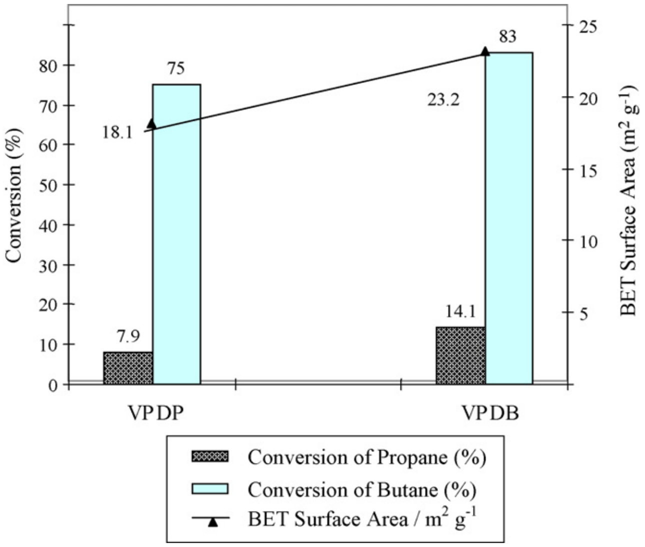

Fig. 9. The relation between conversion (%) and the BET surface area ($m^2\ g^{-1}$) of VPDP and VPDB catalysts in selective oxidation of propane and $n$-butane.

### 3.7. Catalytic oxidation of n-butane

The catalytic performance of the catalysts for butane oxidation to maleic anhydride (MA) has been tested at 613, 643 and 673 K, the latter being a typical operating temperature for VPO catalysts. Fig. 9 shows catalytic performance of VPO as a function of the reaction operating temperature. It is clear from the results obtained that lower operating temperature generally favoured higher selectivity towards MA (Table 4). At 673 K, the $n$-butane conversion for VPDB and VPDP was excellent with 75% and 83%, respectively. As expected, the conversion of $n$-butane decreased with the decreasing of reaction temperature (Fig. 9). The selectivity towards MA increases with decreasing of operating temperature, however, it also noted that there was a decrease in $n$-butane conversion with an increase of MA selectivity for both catalysts tested (Table 4).

Higher activity of VPDB compared to VPDP also contributed by the higher amount of oxygen species removed associated with $V^{IV}$ (~30% more). The role of the active oxygen species ($O^-$) being more clearer now that this oxygen is

Table 4
Catalytic performance of VPDP and VPDB catalysts in $n$-butane oxidation as a function of reaction temperatures[a]

| Reaction temperatures | Conversion of $n$-butane (%) | | MA selectivity (%) | | $CO_2$ selectivity (%) | | CO selectivity (%) | |
|---|---|---|---|---|---|---|---|---|
| | VPDP | VPDB | VPDP | VPDB | VPDP | VPDB | VPDP | VPDB |
| 613 | 28 | 35 | 82 | 76 | 5 | 11 | 13 | 13 |
| 643 | 45 | 58 | 71 | 71 | 13 | 14 | 16 | 15 |
| 673 | 75 | 83 | 64 | 63 | 16 | 18 | 20 | 20 |

[a] GHSV: 2400 $h^{-1}$.

the main factor for hydrocarbon activation which is the main determining step in light hydrocarbon oxidation.

## 4. Conclusions

Activated vanadium phosphate catalysts were obtained by calcining $VOHPO_4 \cdot 0.5H_2O$ precursor in two different hydrocarbons reaction environments, *i.e.* *n*-butane/air and propane/air. Both catalysts exhibited good crystalline with characteristic peaks of pyrophosphate phase. BET surface area showed that the *n*-butane/air calcined catalyst gave higher surface area ($23\ m^2\ g^{-1}$) compared to propane/air calcined catalyst ($18\ m^2\ g^{-1}$). Reduction profiles of both catalysts gave two reduction peaks which correspond to two kinetically different oxygen species which were associated with $V^V$ and $V^{IV}$ phases, respectively. Higher amount of oxygen species associated with $V^{IV}$ was removed from *n*-butane/air calcined catalyst. From the catalytic test for *n*-butane and propane oxidation, *n*-butane calcined catalyst show higher conversion for both hydrocarbons oxidation compared to the propane/air calcined catalyst. The availability and behaviour of active oxygen species ($O^-$) in the catalysts were observed to play the main role in activation of *n*-butane and propane and confirm that this is the main determining step for the oxidation of hydrocarbons .

## References

[1] G. Centi, Catal. Today 16 (1993) 5.

[2] N. Ballarini, F. Cavani, C. Cortelli, S. Ligi, F. Pierelli, F. Triffiro, C. Fumagalli, G. Mazzoni, T. Monti, Top. Catal. 38 (2006) 147.

[3] G.J. Hutchings, J. Mater. Chem. 14 (2004) 3385.

[4] K.C. Waugh, Y.H. Taufiq-Yap, Catal. Today 81 (2003) 215.

[5] J.C. Volta, Top. Catal. 15 (2001) 121.

[6] M. Niwa, Y. Murakami, J. Catal. 76 (1982) 9.

[7] Y.H. Taufiq-Yap, K.P. Tan, K.C. Waugh, M.Z. Hussein, I. Ramli, M.B. Abdul Rahman, Catal. Lett. 89 (2003) 87–93.

[8] F. Cavani, S. Ligi, T. Monti, F. Pierelli, F. Trifirò, S. Albonetti, C. Mazzoni, Catal. Today. 61 (2000) 203.

[9] K. Ait-Lachgar, M. Abon, J.C. Volta, J. Catal. 171 (1997) 383.

[10] P.L. Gai, K. Kourtakis, Science 267 (1995) 661.

[11] M. Abon, K. Bere, A. Tuel, Delichere, J. Catal. 171 (1997) 383.

[12] J.-C. Volta, C.R. Acad. Sci. Paris, Serie IIc, Chemie 3 (2000) 717.

[13] Y. Han, H. Wang, H. Cheng, J. Deng, J. Chem. Soc. Chem. Commun. (1992) 803.

[14] Y.H. Taufiq-Yap, C.S. Saw, R. Irmawati, Catal. Lett. 105 (2005) 103.

[15] Y.H. Taufiq-Yap, C.K. Goh, G.J. Hutchings, N. Dummer, J.K. Bartley, J. Mol. Catal. A: Chem. 260 (2006) 24.